

Aperture Synthesis using Multiple Facilities: Keck Aperture Masking and the IOTA Interferometer

J. D. Monnier^{a,b}, R. Millan-Gabet^{a,c}, P. G. Tuthill^d, W. A. Traub^a, N. P. Carleton^a,
V. Coudé du Foresto^e, W. C. Danchi^f, M. G. Lacasse^a, S. Morel^g, G. Perrin^e,
and I. L. Porro^h

^aHarvard-Smithsonian Center for Astrophysics, 60 Garden St,
Cambridge, MA, 02138, USA

^bUniversity of Michigan, Astronomy Department

^cInterferometry Science Center, California Institute of Technology

^dUniversity of Sydney, Physics Department

^eObservatoire de Paris-Meudon

^fNASA Goddard Space Flight Center

^gEuropean Southern Observatory

^hMassachusetts Institute of Technology

ABSTRACT

As the number of optical interferometers increase, multi-facility observations become both feasible and scientifically interesting. For imaging of complex sources, the capability of increasing (u,v) coverage by using multiple arrays may be necessary for accurately interpreting the fringe visibility and closure phase data. Toward this end, coordinated observations with the IOTA interferometer and Keck aperture masking have been carried out to test techniques for synthesizing images using data from heterogeneous arrays with sparse (u,v) coverage. In particular, we will focus on how the image prior in the Maximum Entropy Method can be used to efficiently incorporate very high spatial frequency information with “low-resolution” data for imaging the generic prototype “Star + Dust Shell” image morphology. Preliminary results using real data for a few dusty evolved stars are presented.

Keywords: optical interferometry, aperture synthesis, imaging, deconvolution, maximum entropy

1. INTRODUCTION

In order to reliably image astronomical objects using interferometry, the resolution of the interferometer must be matched to the size scales present in the source. Stars surrounded by dust shells (such as for young stellar objects and evolved stars) pose a difficult problem for imaging since structures exist on two distinct scales, the extended dust shell and the stellar photosphere. On the other hand, the presence of compact emission is important for “phasing up” long-baseline interferometers relying on fringe-tracking, and hence these sources will be prime targets for imaging with next generation arrays.

Aperture masking on the Keck-I telescope has allowed imaging of dust-enshrouded sources with a resolution of ~ 40 milliarcseconds (mas) in the near-infrared.¹⁻⁴ However, this resolution is not adequate for mapping many sources without higher resolution information from a long-baseline interferometer. However, combining data from multiple interferometers can introduce some additional difficulties, such as uncertainties about source variability in time (for evolved and young stars) and systematic calibration problems due to differences in observing bandpasses or fringe detection techniques.

Send correspondence to J.D.M. E-mail: monnier@umich.edu

Relatively little has thus far been written about combining data from multiple interferometers, especially for imaging work. Monnier et al.⁵ combined mid-infrared speckle interferometry observations (baselines <3 m) with long-baseline ISI interferometer data to constrain a Maximum Entropy reconstruction of two dust shells around the red supergiant NML Cyg. Berger et al.⁶ recently combined data from the IOTA and PTI interferometers to reveal evidence for a previously unknown companion around the partially resolved accretion disk of FU Ori. Data from three interferometers (Mark III, NPOI, PTI) were recently used⁷ for solving the binary orbital parameters of *o* Leo. We expect the use of multiple interferometric facilities for model fitting as well as interferometric imaging will continue grow rapidly, as the new generation of interferometer arrays will have greater overlapping wavelength and baseline coverage than in the past (e.g., CHARA and IOTA, VLTI and iKeck).

In this short paper, we report on some preliminary data reduction and imaging experiments combining Keck aperture masking and IOTA⁸ 2-telescope observations with FLUOR.⁹ The IOTA interferometer was used to measure crucial high resolution information (which probes the stellar photospheric size and flux contribution), essential for interpreting the “low resolution” Keck data (sensitive to the extended dust shell). We reported first results in Monnier et al.¹⁰ and here emphasize more the novel imaging methods under investigation.

2. OBSERVATIONS

Keck aperture masking in 2000 January and 2000 June were complemented by IOTA interferometer observing in 2000 February, 2000 April, and 2000 June. Table 1 lists the targets which were successfully observed by both interferometric experiments at 2.2 μ m. In this paper we will only discuss the imaging experiments of dust-enshrouded sources and not the limb-darkening investigations.

The Keck masking observations and analysis followed standard procedures documented elsewhere.^{3,4} The IOTA observations employed the single-mode fiber coupler FLUOR operating at 2.2 μ m. The data analysis for the FLUOR data did not follow exactly the procedure outlined in Foresto et al.,⁹ and important differences are highlighted in the next section.

3. FLUOR DATA REDUCTION

3.1. CfA Method

By using the natural spatial filtering of single-mode fibers, the FLUOR experiment has reported extraordinarily small error bars for visibility measurements of bright stars.^{11,12} We at the Harvard-Smithsonian Center for Astrophysics (CfA) have developed our own independent data analysis pipeline for FLUOR data following similar procedures⁹ entirely in the IDL analysis environment.

While detailed discussion of the CfA analysis method will be included in a future paper, we summarize the important features here. We follow the standard FLUOR method of recovering the individual telescope fluxes using the photometric channels, P_1 and P_2 . The fringe envelope of an unresolved source should be proportional to $\sqrt{P_1 P_2}$, the proportionality constant being well-known from measurements of the so-called kappa κ matrix.

Table 1. Keck + IOTA Aperture Synthesis Targets Observed

Imaging Dust Shells & Measuring Stellar Diameters	Measurement of Limb-Darkening Effects in the Near-IR
IK Tau	Alp Ori
IRC +10420	R Hya
NML Cyg	R Leo
V Hya	W Hya
VX Sgr	
VY CMa	
HD 62623	

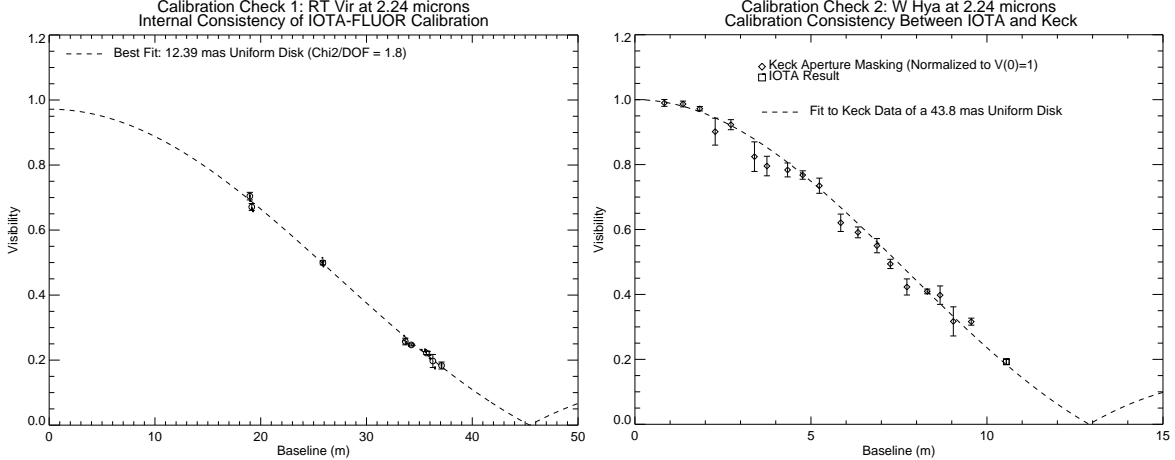


Figure 1. (left panel) a. The combined IOTA-FLUOR data for RT Vir using the preliminary CfA data pipeline. (right panel) b. Testing visibility calibration of Keck aperture masking using a narrow-band $2.24 \mu\text{m}$ filter and IOTA-FLUOR using a broadband K' filter. The data points below 10 m are from Keck-I, while the single data point at 10.5 m is from IOTA; the agreement is quite good.

In the standard FLUOR method, the fringes are normalized on a scan-by-scan basis by dividing by the synthetic fringe envelope formed using $\sqrt{P_1 P_2}$. While attempts are made to avoid biases by smoothing the photometric channels and employing signal-to-noise ratio cuts on the data, we found this method problematic for the faintest targets, since dividing by a noisy signal can introduce uncalibrated bias when the target and calibrator stars are of different brightness. Standard FLUOR analysis requires signal-to-noise ratios of a few in each fringe scan to be properly analyzed, while the CfA method can be used for smaller amplitude signals without introducing bias.

In the CfA method, we instead average the fringe power and the fringe envelope calibration factor separately. This allows us to use many hundred scans (per visit) to accumulate a high signal-to-noise ratio estimate of both the fringe power and a calibration factor before normalization, hence avoiding the possible bias at low signal levels. In each scan, a calibration factor for the fringe *power* is estimated which is proportional to the average ($P_1 P_2$). We have shown that the FLUOR method and the CfA method yield identical results for bright sources, but found the CfA method more robust in the low SNR limit.

All the IOTA-FLUOR data presented here were analyzed using a preliminary version of the CfA data pipeline. The current pipeline has incorporating better understanding of the detector performance, which has led to slight changes in final calibrated visibilities. The data presented here are representative of the quality of final pipeline, and final results using the optimal calibration will be presented in a future paper.

3.2. Validation

Figure 1a shows a calibration study for the source RT Vir (M8III) using a preliminary version of the CfA analysis routines. This source was observed at a range of baselines to test the consistency with a uniform disk (UD) model. We find slight deviations from the best-fitting UD model, possibly caused by residual miscalibration in the data analysis, limb-darkening, time-variability, or the presence of surface structure or circumstellar dust. For now we can conservatively estimate the internal consistency to be at the few percent level per visit (consisting of a few hundred scans acquired in a few minutes). Our preliminary estimate of 12.39 mas is similar to the previous published measurement of 13.06 ± 0.15 mas by Perrin.¹³ While the difference in diameter estimates is statistically significant, it is not possible to assign a definite cause, since many physical effects (as well as miscalibrations) can cause the effective size of the star to change with time (e.g., pulsation or hotspots).

Figure 1b tests the relative systematic calibration between the Keck aperture masking experiment and IOTA-FLUOR. The Mira W Hya was observed using a narrow-band ($\sim 1\%$ bandwidth) filter at Keck, while

IOTA-FLUOR always used a broadband K' (“K-short”) filter. A uniform disk model is plotted through the Keck data (<10 m baselines) and it is seen to be entirely consistent with the IOTA data observed at a slight longer baseline (~ 10.5 m). From extensive observing experience, we have measured the typical Keck calibration error to be $\sim 5\%$ at the longest baselines due to unavoidable changes in seeing conditions between source and calibrator. The IOTA-FLUOR data is calibrated much better than this, thus we are always limited by the calibration of the Keck masking data.

Lastly, we will comment on a few sources of systematic error for the FLUOR data which we do not yet fully understand. We expect there to be calibration corrections if the source and calibrator stars are not the same spectral type due to changes in the shape and width of the fringe envelope when using the power spectrum for estimating fringe power (see discussion and table of correction factors in Foresto et al.⁹). However, these correction factors are seeing-dependent and have not been tabulated for dust-enshrouded stars. Simulations are underway to empirically estimate the magnitude of this effect and will be discussed subsequent papers. Subtleties in the NICMOS camera readout¹⁴ also can introduce small biases in the estimated fringe visibility. Full discussion is beyond the scope of this paper, but effects such as non-linearities and signal persistence for bright sources can cause miscalibrations at the $\sim 1\%$ level.

We note that in the context of this experiment and this paper, the 5% calibration error on the Keck aperture masking data is expected to dominate all the uncompensated IOTA-FLUOR biases.

4. IMAGING DUST SHELLS

4.1. Red Supergiant VY CMa

VY CMa is a red supergiant with an extensive dust shell and intense maser emission. Figure 2a shows the visibility data observed by Keck aperture masking and IOTA in 2000 Jan at $2.2\mu\text{m}$. The Keck data has been smoothed azimuthally below 10 m, but the full 2-dimensional visibility amplitudes are presented in the inset plot. Although there appears to be some dust contribution to the visibility beyond ~ 12 m, the uniform disk diameter can be reliably estimated to be ~ 18 mas.

The Maximum Entropy Method (MEM) was used to image the dust shell around VY CMa using the algorithm of Sivia.¹⁵ The MEM reconstruction using only Keck data is shown in Figure 2b (similar to maps of previous epochs reported by Monnier et al.¹). Careful scrutiny of this image shows that the MEM algorithm has smoothed out the central source in this image; indeed, it appears even slightly elongated. However, from the IOTA data we know the size of this central source to be unresolvable by Keck and further we do expect gross asymmetries in the photosphere based on our understanding of stellar astrophysics.

We can implicitly incorporate the IOTA data through the use of a “MEM prior.” In the absence of useful data, the MEM algorithm will produce a map equal to the MEM prior, discussed in various places.¹⁶ Typically, one uses a flat prior (all pixels in the map are equal) in order not to introduce any *a priori* information. However, in our case we precisely want to include what we know of the stellar contribution into the mapping process.

In the case of VY CMa, we can estimate that the star contributes approximately 33% of the flux, based on the IOTA measurements. We can incorporate this information into the MEM mapping by using a MEM prior consisting of a single pixel containing 33% of the flux with the remaining 67% spread evenly throughly the rest of the field-of-view. Figure 2c shows the MEM reconstruction of the Keck data using this prior. As you can see, the reconstruction of the inner most part of the dust shell is significantly different, suggesting the presence of hot dust much closer to the star than in Figure 2b. Note that the distant dust towards the South is largely unchanged in the images; this dust produces a large closure phase signal in the Keck data and is accurately mapped regardless of MEM prior.

It is interesting to note that (spherically-symmetric) radiative transfer modeling using mid-infrared observations by the ISI interferometer¹⁷ suggested a stellar diameter of 20 mas and an inner dust shell radius of 50 mas (indicated by the dashed circle in Figure 2c) for this source.

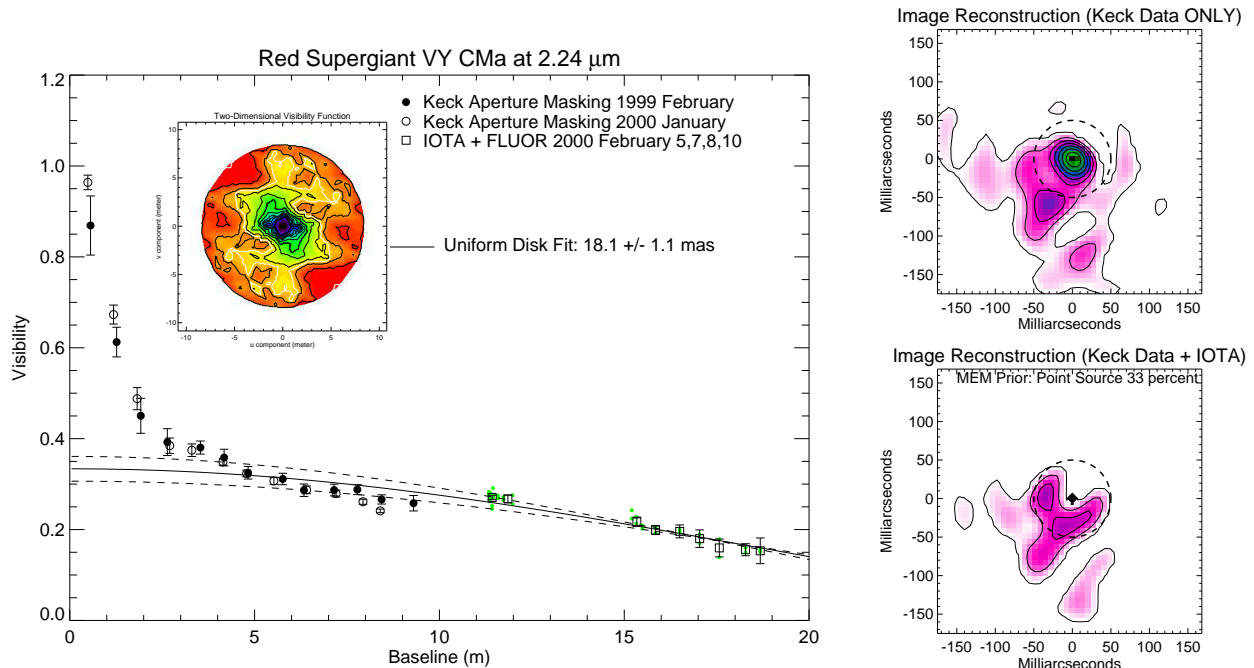


Figure 2. (left panel) a. This figure shows the azimuthally-averaged visibility curve for VY CMA observed by Keck aperture masking at $2.24\mu\text{m}$ and the longer baseline (preliminary) measurements by IOTA. The 2-dimensional visibility function from Keck is included as an inset. A fit to the longest baseline data suggests that VY CMA has UD diameter of ~ 18.1 mas, the first measurement of the size of this prototypical source. (top-right panel) b. Maximum Entropy image reconstruction of the VY CMA dust shell using only Keck data. (bottom-right panel) c. Image reconstruction implicitly including the long-baseline IOTA measurements.

4.2. Dusty Mira IK Tau

IK Tau was one of the first IR sources discovered in the IRC survey (also known as NML Tau¹⁸), yet its stellar diameter is still not known. The Keck-I and IOTA visibility data appear in Figure 3a, in a similar form as Figure 2a. The Keck-I data is entirely dominated by dust shell emission, while the IOTA interferometer appears to have resolved most of the dust and is partially resolving the underlying star itself. Even longer baseline data is required to unambiguously measure the stellar diameter, but we can estimate the stellar size by assuming that the 20 m visibility data is not contaminated by dust emission; the UD fit of the IOTA data yields a stellar diameter of ~ 12.4 mas (with 28% of the $2.2\mu\text{m}$ flux arising from the star).

We can use MEM to image the dust shell using both the flat prior and a MEM prior with a 28% point source, similar to the procedure described above for VY CMA; Figures 3b and 3c show the results. We see that both images show a partial ring of clumpy dust emission around the central source, but the radius of this emission differs by more than a factor of 2 (!) depending on which MEM prior was used. The dashed circle shows the inner radius deduced by ISI measurements nearly 10 years ago.¹⁹ The differences between these images are quite dramatic, because a) the IK Tau dust shell is only partially resolved, and b) because IK Tau has small closure phases (point-symmetric objects are more vulnerable to well-known MEM imaging artifacts¹⁶). We believe the image shown in Figure 3c must most closely resemble the actual circumstellar environment of IK Tau since it incorporates the IOTA long-baseline data. However, definitive tests of these procedures will require a more rigorous set of simulated observations of test cases (currently in preparation).

4.3. Future Work

Other MEM priors could be used for mapping these sources. We are experimenting with a two-step procedure where 1) the azimuthally-averaged visibility curves are fitted with spherically-symmetric radiative transfer

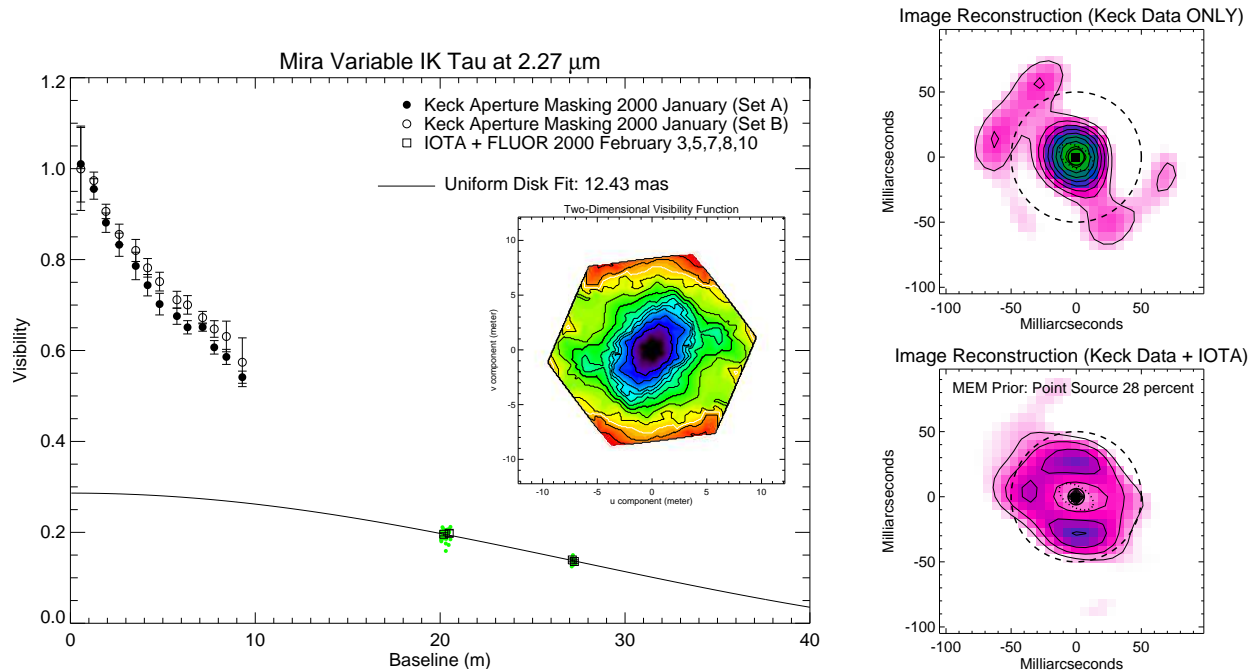


Figure 3. (left panel) a. This figure shows the azimuthally-averaged visibility curve for IK Tau observed by Keck aperture masking at $2.27\mu\text{m}$ and the longer baseline (preliminary) measurements by IOTA. The 2-dimensional visibility function from Keck is included as an inset. A fit to the longest baseline data suggests that IK Tau has a UD diameter of ~ 12.4 mas, the first measurement of the size of this prototypical source. (top-right panel) b. Maximum Entropy image reconstruction of the IK Tau dust shell using only Keck data. (bottom-right panel) c. Image reconstruction implicitly including the long-baseline IOTA measurements.

model, and 2) the synthetic image of this dust shell is used as the MEM prior. This procedure should allow both the average radius of dust emission to be accurately estimated, but the MEM imaging will allow the clumpy structure encoded in the non-zero closure phases to be reconstructed.

The use of MEM priors is clearly only an *ad hoc* way of incorporating the IOTA data into the mapping process, and is not intellectually satisfying. More general and theoretically well-motivated methods might include multi-resolution techniques based on recent innovations in deconvolution theory, such as pixons²⁰ or wavelets.²¹ Adopting this work for image reconstructions using sparsely-sampled visibility amplitudes and closure phases should pose an interesting challenge.

5. CONCLUSIONS

There are a number of interesting conclusions we can draw from this preliminary analysis.

- Independent data analysis pipeline confirms that the FLUOR combiner on IOTA produces (conservatively) a few percent statistical errors (per visit) for bright sources under average to good seeing conditions; this error can be further reduced through multiple observations. Unfortunately, systematic errors, due to color differences between source and calibrator stars and due to subtle camera effects, can also be of this magnitude for faint dusty objects; effective calibration procedures are still being explored.
- By combining data from IOTA and Keck aperture masking, we have been able to measure the stellar diameters of prototypical dust-enshrouded stars. It has previously been impossible to spatially separate dust shell from photospheric emission.

- For the common case that a circumstellar dust shell is only partially resolved, good knowledge of the size and flux contribution of the underlying star can be used to facilitate a reliable image reconstruction.
- Development of special image reconstruction algorithms is needed to properly handle sparsely-sampled optical interferometry data.

REFERENCES

1. J. D. Monnier, P. G. Tuthill, B. Lopez, P. Cruzalebes, W. C. Danchi, and C. A. Haniff, "The Last Gasp of VY Canis Majoris: Aperture Synthesis and Adaptive Optics Imagery," *ApJ* **512**, pp. 351–361, Feb. 1999.
2. P. G. Tuthill, J. D. Monnier, and W. C. Danchi, "A dusty pinwheel nebula around the massive star WR 104," *Nature* **398**, pp. 487–489, 1999.
3. J. D. Monnier, *Infrared Interferometry and Spectroscopy of Circumstellar Envelopes*. PhD thesis, University of California at Berkeley, 1999.
4. P. G. Tuthill, J. D. Monnier, W. C. Danchi, E. H. Wishnow, and C. A. Haniff, "Michelson Interferometry with the Keck I Telescope," *PASP* **112**, pp. 555–565, Apr. 2000.
5. J. D. Monnier, M. Bester, W. C. Danchi, M. A. Johnson, E. A. Lipman, C. H. Townes, P. G. Tuthill, T. R. Geballe, D. Nishimoto, and P. W. Kervin, "Nonuniform Dust Outflow Observed around Infrared Object NML Cygni," *ApJ* **481**, pp. 420–+, May 1997.
6. J. Berger, F. Malbet, M. M. Colavita, D. Segransan, R. Millan-Gabet, and W. A. Traub, "New insights into the nature of the circumstellar environment of FU Ori," in *Proc. SPIE Vol. 4006, p. 597-604, Interferometry in Optical Astronomy, Pierre J. Lena; Andreas Quirrenbach; Eds., 4006*, pp. 597–604, July 2000.
7. C. A. Hummel, J.-M. Carquillat, N. Ginestet, R. F. Griffin, A. F. Boden, A. R. Hajian, D. Mozurkewich, and T. E. Nordgren, "Orbital and Stellar Parameters of Omicron Leonis from Spectroscopy and Interferometry," *AJ* **121**, pp. 1623–1635, Mar. 2001.
8. N. P. Carleton, W. A. Traub, M. G. Lacasse, P. Nisenson, M. R. Pearlman, R. D. Reasenberg, X. Xu, C. M. Coldwell, A. Panasyuk, J. A. Benson, C. Papaliolios, R. Predmore, F. P. Schloerb, H. M. Dyck, and D. M. Gibson, "Current status of the iota interferometer," *Proc. SPIE* **2200**, pp. 152–165, June 1994.
9. V. Coude Du Foresto, S. Ridgway, and J. . Mariotti, "Deriving object visibilities from interferograms obtained with a fiber stellar interferometer," *A&AS* **121**, pp. 379–392, Feb. 1997.
10. J. D. Monnier, R. Millan-Gabet, P. G. Tuthill, W. Traub, N. Carleton, V. Coude du Foresto, W. C. Danchi, M. Lacasse, S. Morel, G. Perrin, and I. Porro, "Aperture Synthesis with the IOTA Interferometer plus Keck-I Aperture Masking," *American Astronomical Society Meeting* **198**, pp. 0–+, May 2001.
11. G. Perrin, V. Coude Du Foresto, S. T. Ridgway, J.-M. Mariotti, W. A. Traub, N. P. Carleton, and M. G. Lacasse, "Extension of the effective temperature scale of giants to types later than M6," *A&A* **331**, pp. 619–626, Mar. 1998.
12. G. Perrin, V. Coude du Foresto, S. T. Ridgway, B. Mennesson, C. Ruilier, J.-M. Mariotti, W. A. Traub, and M. G. Lacasse, "Interferometric observations of R Leonis in the K band. First direct detection of the photospheric pulsation and study of the atmospheric intensity distribution," *A&A* **345**, pp. 221–232, May 1999.
13. G. Perrin, *Une unité de recombinaison à fibres pour l'interféromètre IOTA. Application à l'étude des étoiles de type tardif*. PhD thesis, L'Université de Paris, 1996.
14. R. Millan-Gabet, F. P. Schloerb, W. A. Traub, and N. P. Carleton, "A NICMOS3 Camera for Fringe Detection at the IOTA Interferometer," *PASP* **111**, pp. 238–245, Feb. 1999.
15. D. Sivia, *Phase Extension Methods*. PhD thesis, Cambridge University, 1987.
16. R. Narayan and R. Nityananda, "Maximum entropy image restoration in astronomy," *ARA&A* **24**, pp. 127–170, 1986.
17. J. D. Monnier, W. C. Danchi, D. S. Hale, E. A. Lipman, P. G. Tuthill, and C. H. Townes, "Mid-Infrared Interferometry on Spectral Lines. II. Continuum (Dust) Emission Around IRC +10216 and VY Canis Majoris," *ApJ* **543**, pp. 861–867, Nov. 2000.
18. G. Neugebauer, D. E. Martz, and R. B. Leighton, "Observations of Extremely Cool Stars.," *ApJ* **142**, pp. 399–+, July 1965.

19. W. C. Danchi, M. Bester, C. G. Degiacomi, L. J. Greenhill, and C. H. Townes, "Characteristics of dust shells around 13 late-type stars," *AJ* **107**, pp. 1469–1513, Apr. 1994.
20. R. K. Pina and R. C. Puetter, "Bayesian image reconstruction - The pixon and optimal image modeling," *PASP* **105**, pp. 630–637, June 1993.
21. J.-L. Starck, F. Murtagh, P. Querre, and F. Bonnarel, "Entropy and astronomical data analysis: Perspectives from multiresolution analysis," *A&A* **368**, pp. 730–746, Mar. 2001.